Drug Design, Development and Therapy

Dovepress
open access to scientific and medical research

Open Access Full Text Article

ORIGINAL RESEARCH

Mechanisms of Action of *Potentilla discolor* Bunge in Type 2 Diabetes Mellitus Based on Network Pharmacology and Experimental Verification in *Drosophila*

Yinghong Li[1,*], Fanwu Wu[1,*], Jianbo Zhang[1], Ye Xu[1], Hong Chang[1], Yueyue Yu[1], Chunhua Jiang[1], Xiujuan Gao[1], Huijuan Liu[1], Zhen Chen[2], Chenxi Wu[1], Ji-An Li[1,3]

[1]Hebei Key Laboratory of Integrated Traditional Chinese and Western Medicine for Diabetes and Its Complications, College of Traditional Chinese Medicine, North China University of Science and Technology, Tangshan, People's Republic of China; [2]Oriental Herbs KFT, Budapest, Hungary; [3]School of Public Health, North China University of Science and Technology, Tangshan, People's Republic of China

*These authors contributed equally to this work

Correspondence: Chenxi Wu; Ji-An Li, Tel +86-15930951086, Fax +86-03158805765, Email chenxi.wu@ncst.edu.cn; JianLi@ncst.edu.cn

Purpose: Type 2 diabetes mellitus (T2DM) is associated with reduced insulin uptake and glucose metabolic capacity. *Potentilla discolor* Bunge (PDB) has been used to treat T2DM; however, the fundamental biological mechanisms remain unclear. This study aimed to understand the active ingredients, potential targets, and underlying mechanisms through which PDB treats T2DM.

Methods: Components and action targets were predicted using network pharmacology and molecular docking analyses. PDB extracts were prepared and validated through pharmacological intervention in a *Cg*>InR^{K1409A} diabetes *Drosophila* model. Network pharmacology and molecular docking analyses were used to identify the key components and core targets of PDB in the treatment of T2DM, which were subsequently verified in animal experiments.

Results: Network pharmacology analysis revealed five effective compounds made up of 107 T2DM-related therapeutic targets and seven protein–protein interaction network core molecules. Molecular docking results showed that quercetin has a strong preference for interleukin-1 beta (IL1B), IL6, RAC-alpha serine/threonine-protein kinase 1 (AKT1), and cellular tumor antigen p53; kaempferol exhibited superior binding to tumor necrosis factor and AKT1; β-sitosterol demonstrated pronounced binding to Caspase-3 (CASP3). High-performance liquid chromatography data quantified quercetin, kaempferol, and β-sitosterol at proportions of 0.030%, 0.025%, and 0.076%, respectively. The animal experiments revealed that PDB had no effect on the development, viability, or fertility of *Drosophila* and it ameliorated glycolipid metabolism disorders in the diabetes *Cg*>InR^{K1409A} fly. Furthermore, PDB improved the body size and weight of *Drosophila*, suggesting its potential to alleviate insulin resistance. Moreover, PDB improved Akt phosphorylation and suppressed CASP3 activity to improve insulin resistance in *Drosophila* with T2DM.

Conclusion: Our findings suggest that PDB ameliorates diabetes metabolism disorders in the fly model by enhancing Akt activity and suppressing CASP3 expression. This will facilitate the development of key drug targets and a potential therapeutic strategy for the clinical treatment of T2DM and related metabolic diseases.

Keywords: *Potentilla discolor* Bunge, T2DM, network pharmacology, molecular docking, *Drosophila*

Introduction

Diabetes mellitus (DM) is a persistent metabolic disorder characterized by elevated blood glucose levels, presenting a complex pathogenesis and substantial risks.[1] In particular, type 2 diabetes mellitus (T2DM) dominates, contributing to >90% of all diabetes cases through insulin resistance (IR) and β-cell dysfunction.[2] T2DM emerges when declining insulin efficacy triggers excess secretion, leading to hyperinsulinemia attributed to the mismatch between insulin resistance and inadequate compensatory insulin secretion.[3] Although conventional treatments like metformin, GLP-1

Received: 27 October 2023
Accepted: 7 March 2024
Published: 11 March 2024

Graphical Abstract

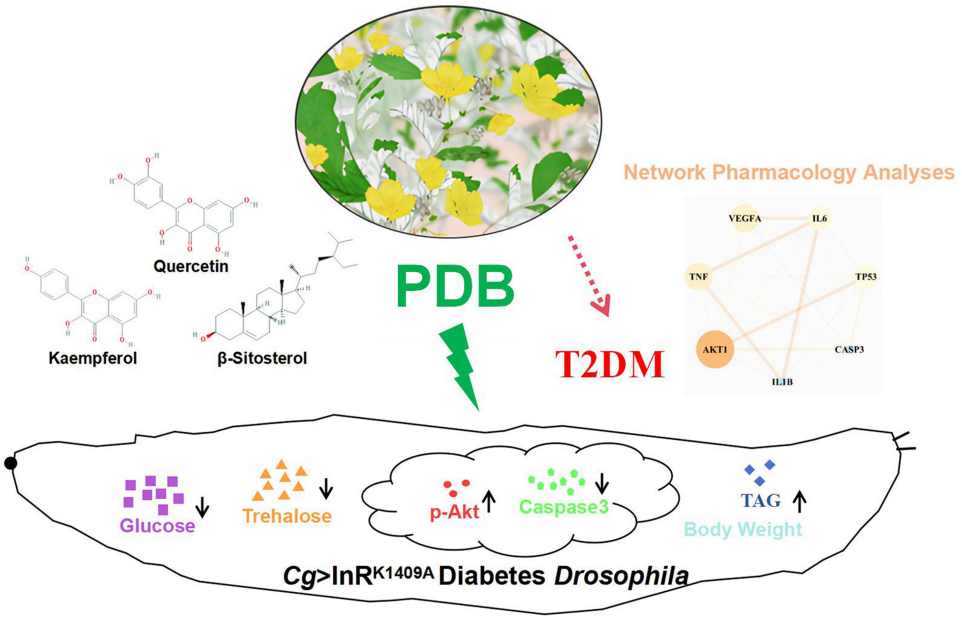

receptor agonists, and insulin mitigate T2DM, challenges such as drug resistance and adverse reactions, including weight gain, hypoglycemia, gastrointestinal effects, and cardiovascular disease, persist. Traditional Chinese medicine (TCM), featuring multi-link, -target, and -pathway activation mechanisms, has demonstrated notable therapeutic effects in T2DM, with an excellent safety profile, rendering it of high research value.

Potentilla discolor Bunge (PDB) is a perennial herb belonging to the Rosaceae family with a broad distribution across Asia. It has a mild sweet-bitter taste.[4] It is typically used in traditional medicine for its anti-inflammatory, heat-clearing, and haemostatic effects. PDB is mainly utilised to treat carbuncles, sores, damp-heat diarrhoea, lung-heat cough/asthma, and various haemorrhagic fevers.[5] It contains various effective components such as quercetin, caffeic acid, kaempferol, protocatechuic acid, and β-sitosterol,[6,7] which exhibit antibacterial, anti-inflammatory, antioxidative, antidiarrheal, anti-tumor, and immunosuppressive effects. Notably, PDB has shown a substantial effect on T2DM.[8–10] Despite the known impact of PDB on insulin resistance and blood sugar levels,[11,12] its intricate mechanisms on insulin sensitivity, glucose–lipid metabolism, and oxidative stress are largely unknown and necessitate further investigation. In addition, the effective components, action targets, and molecular mechanisms of PDB in the treatment of T2DM have not yet been elucidated and warrant further investigation.

With the advantages of rapid reproduction, large numbers of offspring, simple genetic manipulation, and no stringent ethical issues,[13] *Drosophila melanogaster* has emerged as an ideal experimental organism for investigating the pharmacodynamics of glucose and lipid metabolism disorders, as well as related diseases.[14,15] More than 70% of human disease genes have direct homologs in fruit flies, and many metabolic-related biochemical pathways, signaling pathways, and regulatory proteins are conserved in both fruit flies and humans[16.] In contrast to the high-calorie diet-induced models of diabetes in mammals or flies,[17–19] the *Cg*>InR^{K1409A} diabetic fly model we employed in this study was developed using the GAL4/UAS expression technique, which was used to specifically express a dominantly negative form of the insulin receptor (InR) (*UAS*-InR^{K1409A}) in the fat body (equivalent to the mammalian adipose tissue and liver), thus interfering with the physiological function of the endogenous InR to cause IR and decrease the activity of insulin signaling. Therefore, this fly model may be more suitable for exploring the effects of drugs or active ingredients in treating diabetes and related diseases.

As a modern research method for exploring the relationship between drugs and diseases, Network pharmacology is a holistic and systematic approach that focuses on the interactions between drugs and targets, ensuring consistency with the holistic view, syndrome differentiation, and treatment principles of TCM, thus providing researchers with novel ideas and methods for investigation.[20] Thus, our study employed network pharmacology and molecular docking analyses to preliminarily identify the key components and core targets of PDB in treating T2DM. Next, we developed the *Cg*>InR^{K1409A} *Drosophila* diabetic model to further validate the regulatory effects among the core components and targets in vivo with the aim of exploring the underlaying molecular mechanisms of PDB extract in treating T2DM. Together, the findings reported herein provide experimental evidence and a theoretical basis for the clinical application of PDB in treating T2DM-related diseases.

Materials and Methods

Screening for Active Components and Action Targets of TCM

Screening for active ingredients and targets was performed using the TCMSP database (Supplementary Table 1) with "Fanbaicao" as the Chinese input and oral bioavailability (OB) ≥ 30% and drug-likeness (DL) ≥ 0.18 as the inclusion criteria.[21] UniProt was used to retrieve the standardized protein names and genes associated with the identified targets.[22] Both active components and related target gene names were then imported into Cytoscape V3.7.1 to construct an active component-target network.

Screening and Analysis of Intersecting TCM-Disease Targets

Disease targets were retrieved from OMIM, GeneCards, PharmGKB, TTD, and DrugBank (Supplementary Table 1) using "Type 2 Diabetes" as the query keyword, with the intersecting results considered as disease targets. Targets were then uploaded to the bioinformatics website for online analysis, and the obtained intersecting targets were used to construct a Venn diagram.

Construction of a Protein-Protein Interaction (PPI) Network

A PPI network was generated by importing the intersection targets into the STRING database, with the protein type set to "homo sapiens" and the medium confidence set to 0.4. The results were downloaded in TSV format and imported into Cytoscape V3.7.1. The topology of the PPI network was analyzed using the "Network Analyzer" function, and targets whose degree, betweenness, and closeness centrality were greater than or equal to the median were identified. This process was repeated in triplicate, and the results were used to construct a network of key targets.

Gene Ontology (GO) and Kyoto Encyclopaedia of Genes and Genomes (KEGG) Enrichment Analysis

The TCM-disease intersection targets were input into the DAVID database with the species set to "H. sapiens". GO functional analysis was performed on the top 10 targets and KEGG pathway enrichment analysis on the top 30 items ranked according to *P* values. The results were graphically presented using the bioinformatics website.

Molecular Docking Analysis

According to the sequence numbers of key targets identified in the UniProt database, three-dimensional images were downloaded from the PDB database and saved in the PDB format. Subsequently, the file was imported into Pymol, wherein non-polar hydrogens were introduced and water molecules and small molecular ligands were deleted to obtain the intended receptors. The three-dimensional structural diagrams of the main active components of PDB were downloaded from the TCMSP database and saved in mol2 format. The ligands and receptors were then imported into AutoDockTools V1.5.6 for molecular docking analysis and visual presentation.

PDB Extract Preparation

PDB samples were purchased from Beijing Tongrentang Tangshan Chain Store Drug Store Co., Ltd. (Beijing, China, No. 200401) and authenticated by Professor Wu Fanwu at the North China University of Science and Technology. PDB

extraction was performed according to the method: (1) PDB whole plant was ground, and 80 g was packed into a gauze bag that was soaked in 1200 mL 70% ethanol for 48 h at 4 °C; (2) the liquid outside the gauze bag was filtered and the supernatant collected via centrifugation at 25 °C and 4200 ×*g* for 2 h; (3) the remaining residue was boiled in 1 L deionized water for 1 h, cooled, and centrifuged at 4200 ×*g* for 2 h; and (4) the supernatants from the above two steps were combined, filtered (0.45 μm), and diluted to obtain mother liquor at a concentration of 0.8 g/mL.

High-Performance Liquid Chromatography (HPLC) Analysis

HPLC to determine the representative components of PDB extract was performed using the LC-20A system (Shimadzu, Japan) with an Agilent Eclipse XDB-C18 column (4.6 × 250 mm, 5 μm) (Agilent Technologies, Inc., CA, USA). The mobile phase flow rate was set at 1 mL/min and the column temperature was 35 ± 1 °C. Standards (quercetin, kaempferol, and β-sitosterol) were obtained from the National Institute for Food and Drug Control (NIFDC). Detection was performed at a wavelength of 210 nm for β-sitosterol with methanol (A) and water (B) (A: B = 98:2) as the mobile phase, while that of quercetin and kaempferol was performed at 360 nm, with acetonitrile (C) and 0.2% phosphoric acid solution (D) (C: D = 15:85) as the mobile phase.

Drosophila Strains and Genetics

Drosophila melanogaster was grown at 25 °C under 55–65% humidity in a 12-h light/dark cycle with a culture medium comprising 50 g sucrose, 60 g cornmeal, 10 g agar, 30 g yeast, 6 mL propionic acid, and 1 L purified water. *Drosophila* strains w^{1118} (#3605), *Cg*-GAL4 (#7011), and *UAS*-InR^{K1409A} (#8253) were purchased from the Bloomington *Drosophila* Stock Center (Indiana University, IN, USA). The prepared PDB extract mother liquor or the dissolved metformin mother liquor was introduced into double-distilled water and used to configure the medium with the specific concentration required for each experimental group. The fruit flies in the metformin positive control (Met) and PDB treatment groups were fed culture medium containing Met (10 mM) or PDB (2.0, 4.0, 8.0, 16.0, and 32.0 mg/mL), respectively.[23] Healthy, unmated female and male parents were randomly assigned to groups for hybridization.

Developmental and Fertility Assay

We selected 30 female and 20 male fruit fly parents from the w^{1118} strain for crossbreeding and allowed them to lay eggs in a conventional culture medium or PDB-amended culture medium. Healthy larvae were selected 24 h after egg laying and placed in the new corresponding medium at 30 animals/tube. The numbers of pupae and fledged offspring in each tube were recorded every 4 h, and the results were used to plot a developmental curve and calculate viability.[24] For the fertility assay, male or female F1 flies from each group were successfully mated with healthy virgin w^{1118} males or females. The F1 flies were classified as fertile or sterile depending on whether descendants were produced.[25]

Measurement of Metabolites

Samples of third-instar larvae in each group were collected, washed with phosphate-buffered saline (PBS) solution, dried, and placed on slides. Haemolymph released by cuticle tearing was collected immediately, diluted by a factor of 20 with cold PBS, and measured for glucose content using HK reagent (Sigma-Aldrich, St. Louis, MO, USA, #G3293), according to Cao et al.[23] Trehalose measurement was performed by first conducting overnight digestion with porcine trehalase (Sigma-Aldrich, #T8778) at 37 °C, followed by the same procedure used for glucose measurements. The haemolymph trehalose concentration was determined by subtracting the value of free glucose from that of an untreated sample.

The third-instar larvae of each group were collected, washed with PBS, dried, placed in liquid nitrogen for rapid freezing, lysed with 100 μL of cold 0.05% PBST (PBS + 0.05% Tween-20), and ground. The powdered samples were heated at 75 °C for 10 min to remove endogenous enzymes and then cooled to 25 °C. Next, 10 μL of the homogenate was mixed with 10 μL of triglyceride (TAG) reagent (Sigma-Aldrich, #T2449) spiked with lipase, incubated for 1 h at 37 °C, and centrifuged for 3 min at 12,700 rpm. The supernatant (10 μL) was then removed and allowed to react with the free glycerol reagent (Sigma-Aldrich, #F6428), and absorbance was measured at 540 nm to determine the TAG concentration. Another 10 μL aliquot of homogenate was then centrifuged at 12,700 rpm for 3 min (without lipase treatment), and the supernatant was analysed to determine the free glycerol concentration. The TAG concentration in each sample was

determined by subtracting the amount of free glycerol from that of the untreated samples. Homogenate (10 μL) was removed and measured for protein content using the bicinchoninic acid assay (Beyotime, China, #P0010). The resulting TAG per fly was normalized to obtain the soluble protein per fly.[26]

Food Intake

Early third-instar larvae were washed with PBS and subjected to starvation for 2 h (the diet contained 0.8% agar in PBS) and fed 0.05% brilliant blue FCF (Blue-9) for 20 min, washed with PBS, dried, and ground in 100 μL of lysis buffer (PBS + 0.1% Triton X-100). The resulting mixture was subjected to a previously described protocol.[23]

Immunofluorescence

The dissected larval tissues were fixed in 4% formaldehyde for 20 min at 20 °C, washed thrice in 0.3% (v/v) PBST, and stained with primary antibodies overnight at 4 °C and secondary antibodies at 25°C for 4 h. Mouse anti-Dlg1 (1:100, Developmental Studies Hybridoma Bank, #4F3 anti-discs large), rabbit anti-Akt [1:400, Cell signaling technology, MA, USA (CST), #4691], rabbit anti-p-Akt (1:400, CST, #4060), rabbit anti-cleaved Caspase 3 (1:400, CST, #9661) goat anti-mouse cyanine3 (Cy3) (1:1000, Life Technologies, CA, USA, #A10521), and goat anti-rabbit Alexa 488 (1:1000, CST, #4412) were used. Vectashield medium (Vector Laboratories, CA, USA, #H-1500) with 4′,6-diamidino-2- phenylindole was used for mounting.

Western Blotting

Whole larvae were lysed in radioimmunoprecipitation assay buffer (Beyotime, #P0013) with phosphatase inhibitor cocktail A (Beyotime, #P1082) and PMSF. Equal amounts of protein (10–30 μg, measured using bicinchoninic acid assay) were separated using sodium dodecyl sulfate-polyacrylamide gel electrophoresis, transferred to a polyvinylidene fluoride membrane, and subjected to standard WB. Rabbit anti-Akt (1:1000, CST, #4691), rabbit anti-p-Akt (1:2000, CST, #4060), rabbit anti-β-actin (1:1000, CST, #4967), and goat anti-rabbit IgG (H+L, HRP) (1:10,000, SeraCare Life Sciences Inc., MA, USA, #5220-0336) were used for incubation.

Statistical Analysis

All data were verified using at least three independent experiments. GraphPad Prism V8.0 software was used to process the results and produce bar graphs or line charts. One-way analysis of variance (ANOVA) was employed using Bonferroni's multiple comparison test or the chi-squared test. The central values were taken as the mean, and error bars indicate the standard deviation (mean ± SD). Statistical significance was set at $P < 0.05$ and the central value was considered the mean.

Results

Screening for Antidiabetic Targets

The entire PDB plant (Figure 1a and b) is utilized in clinical practice. The active constituents and antidiabetic mechanism for PDB were identified using the TCMSP database, which includes key information on the components, molecular structures, key ADME (absorption, distribution, metabolism, and excretion) parameters, component-target interactions, and relevant diseases for all TCM herbal drugs listed in the Chinese Pharmacopoeia, thus meeting the requirements of network pharmacology evaluation.[27]

Utilizing TCMSP data led to the identification of 17 chemical components in PDB (Supplementary Table 2), of which five met the requirements of OB ≥30% and DL ≥0.18 (Table 1): β-sitosterol, sitosterol, kaempferol, (+)-catechin, and quercetin. Other ingredients, such as lignoceric and ursolic acids, were excluded according to their OB and DL values. The five active components and corresponding 170 targets (Supplementary Table 3) were imported into Cytoscape V3.7.1 to construct a drug-active component-target network relationship diagram (Figure 1c), which included 176 nodes and 249 edges (mutual interactions between active components and targets). Then, OMIM, GeneCards, DrugBank, PharmGKB, and TTD were used to obtain 1556 T2DM disease targets (Figure 1d), and duplicates were removed,

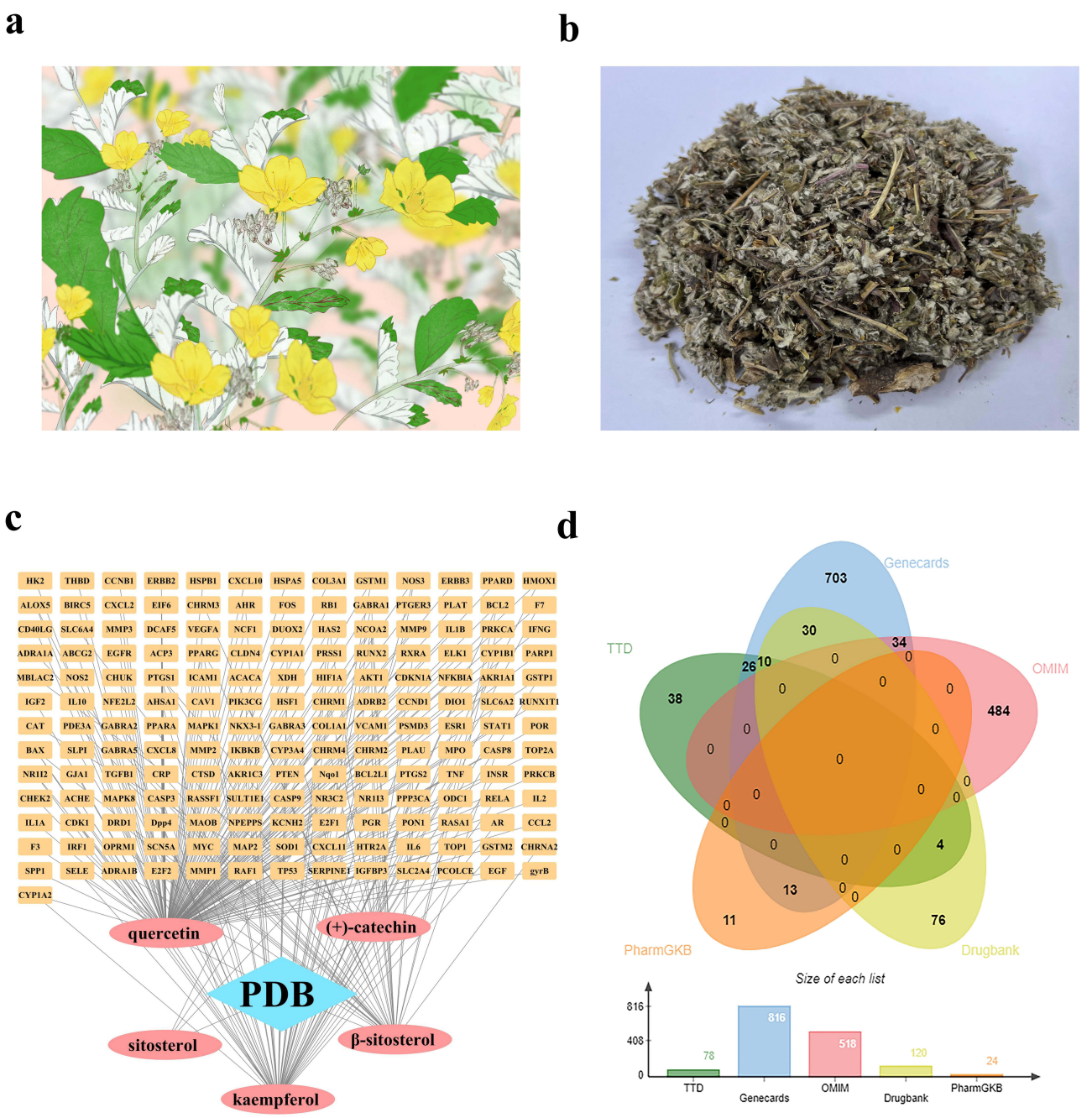

Figure 1 Bioinformatic analysis of PDB ingredients and disease targets. Drawing (**a**) and photograph (**b**) of PDB. (**c**) Active component-target network of PDB. The blue diamond represents PDB, pink circles are the active components, orange rectangles indicate targets, and connecting lines indicate relationships among linked nodes. (**d**) Disease database union of OMIM, GeneCards, PharmGKB, TTD, and DrugBank.

resulting in 1429 T2DM-related disease targets. The obtained component and disease targets were then uploaded to the bioinformatics website for analysis, and 107 potential targets for treating T2DM were identified (Figure 2a).

PPI Network Analysis

To analyze the drug-disease intersection targets, we generated a PPI network diagram using Cytoscape V3.7.1 by importing the 107 target genes (107 nodes, 2024 edges, and an average of 37.8 nodes) into the STRING database (Figure 2b). Triplicate topological analysis (Figure 2c–f) revealed seven key targets [Vascular endothelial growth factor A (VEGFA), Interleukin-1

Table 1 List of Chemical Components That Met the OB and DL Limits with Their Corresponding Molecule Name and ID

Mol ID[a]	Molecule Name	OB[b] (%)	DL[c]
MOL000358	β-sitosterol	36.91	0.75
MOL000359	Sitosterol	36.91	0.75
MOL000422	Kaempferol	41.88	0.24
MOL000492	(+)-Catechin	54.83	0.24
MOL000098	Quercetin	46.43	0.28

Notes: [a]Molecular identification; [b]oral bioavailability (OB) ≥ 30%, [c]drug-likeness (DL) ≥ 0.18.

beta (IL1B), tumor necrosis factor (TNF), Interleukin-6 (IL6), Caspase-3 (CASP3), RAC-alpha serine/threonine-protein kinase (AKT1), and cellular tumor antigen p53 (TP53)] (Table 2) that may be central in treating T2DM.

GO and KEGG Enrichment Analysis

To investigate the cell functions that are primarily impacted by the 107 candidate targets, GO enrichment analysis was performed, with biological processes, molecular functions, and cellular components analysis resulting in 705 entries ($P < 0.05$) (Supplementary Figure 1a). The 550 biological process entries included the cytokine-mediated signaling pathway, hypoxia response, and lipopolysaccharide response; the 50 cellular component entries included membrane raft, transcription factor complex, and mitochondrial outer membrane; the 105 molecular function entries included enzyme binding, RNA polymerase II transcription factor activity, ligand-activated sequence-specific DNA binding RNA, and transcription coactivator binding. The KEGG pathway enrichment analysis on the 107 intersection target genes resulted in a total of 161 pathways ($P < 0.05$), from which the top 30 pathways related to T2DM were identified (Supplementary Figure 1b and Supplementary Table 4), including the AGE-RAGE, PI3K-Akt, and TNF pathways.

Molecular Docking Analysis

To further clarify the possible potential interactions between the active components and core targets, seven core targets (VEGFA, IL1B, TNF, IL6, CASP3, AKT1, and TP53) and their corresponding chemical compounds (quercetin, kaempferol, and β-sitosterol) were screened via molecular docking analysis (Table 3), and results with a binding energy of < −5.0 kcal/mol were visualised.[28]

We selected certain interactions with remarkable affinity, namely IL1B-quercetin (−6.13), IL6-quercetin (−5.15), AKT1-quercetin (−6.48), TP53-quercetin (−5.76), TNF-kaempferol (−6.18), AKT1-kaempferol (−6.85), and CASP3-β-sitosterol (−7.1). The Pymol tool facilitated the in-depth examination of receptor–ligand interactions (Figure 3). These findings highlight the potent binding capabilities of these active constituents to T2DM-associated target genes. Specifically, quercetin exhibited a strong preference for IL1B, IL6, AKT1, and TP53; kaempferol exhibited superior binding to TNF and AKT1; β-sitosterol demonstrated pronounced binding to CASP3. Notably, β-sitosterol displayed the most favorable binding to CASP3, highlighting its strong binding activity. These data verify the action of the key identified PDB components in regulating IL1B, IL6, TP53, AKT1, and CASP3 in T2DM.

Analysis of Representative Compounds Using HPLC

PDB extract was prepared, and its quality was checked. Three representative compounds were selected as quality standards according to the results of the molecular docking analysis. Compared to the peaks of the standard controls (Supplementary Figure S2), distinguished peaks visualised using HPLC (Figure 4) indicated quercetin, kaempferol, and β-sitosterol at proportions of 0.030%, 0.025%, and 0.076%, respectively (Table 4). The results suggested that PDB contained the necessary active components for further in vivo study.

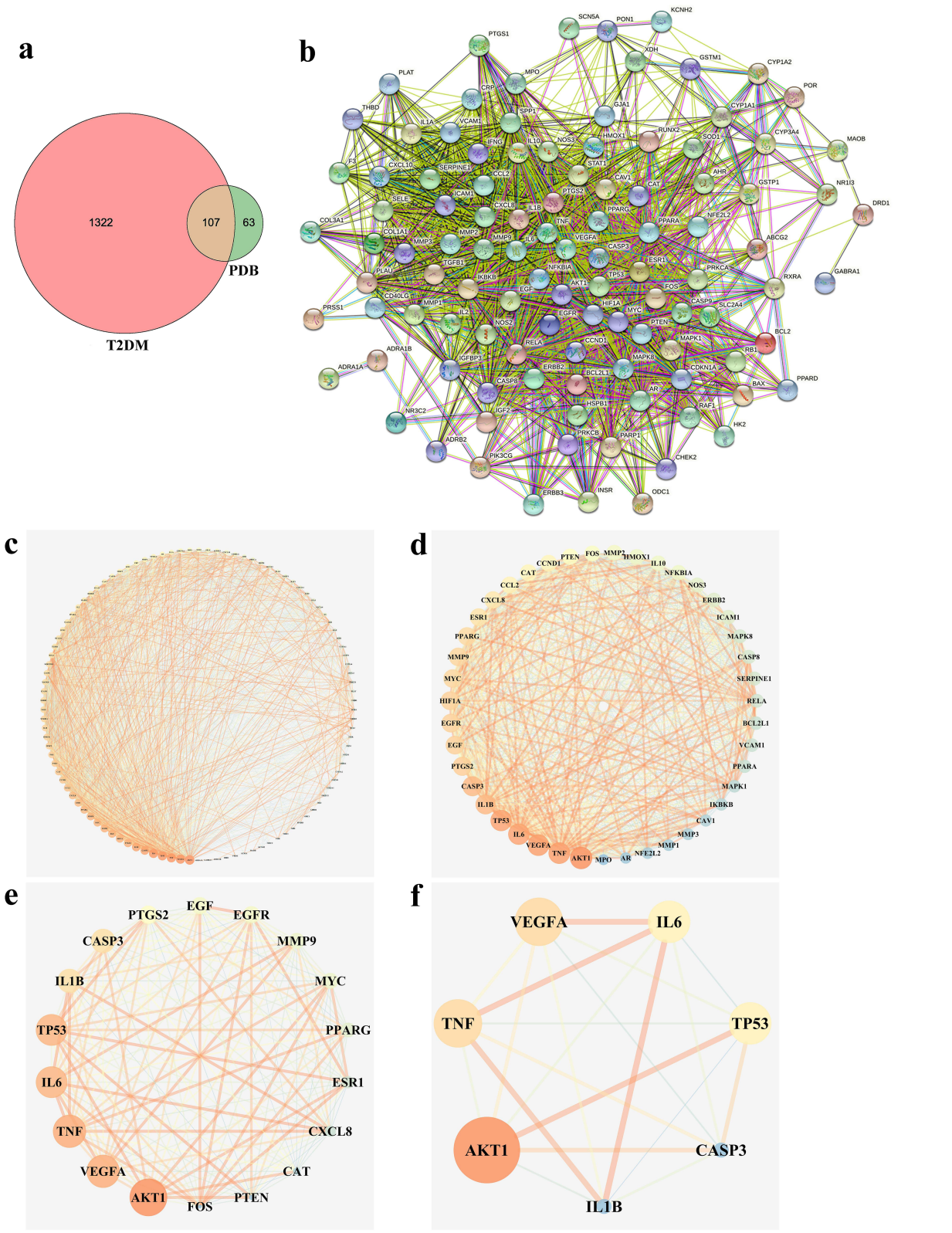

Figure 2 PDB-T2DM intersecting targets and PPI network analysis. (**a**) Venn diagram of PDB-T2DM intersection targets. The pink circle represents T2DM targets. The green circle represents PDB targets and orange segment represents intersecting targets. (**b**) Protein-protein interaction (PPI) analysis. Each node represents one protein. Lines represent associations between nodes. (**c–f**) Core proteins in the Semen PDB-T2DM PPI network. Screening criteria were set according to the median of degree, betweenness, and closeness.

Table 2 Identified Key Targets Using PPI Network Analysis That May Treat T2DM[a]

Name[b]	Betweenness Centrality	Closeness Centrality	Degree
VEGFA	0.02499544	0.78947368	81
IL1B	0.02101123	0.76642336	75
TNF	0.03439745	0.80152672	81
IL6	0.03327964	0.79545455	80
CASP3	0.02448601	0.75539568	75
AKT1	0.03718646	0.8203125	84
TP53	0.02396819	0.78358209	80

Notes: [a]Targets whose degree, betweenness, and closeness centrality greater than or equal to the median.
Abbreviation: PPI, protein–protein interaction; T2DM, type 2 diabetes mellitus, [b]VEGFA, Vascular endothelial growth factor A; IL1B, Interleukin-1 beta; TNF, tumor necrosis factor; IL6, Interleukin-6; CASP3, Caspase-3; AKT1, RAC-alpha serine/threonine-protein kinase; TP53, Cellular tumor antigen p53.

Table 3 Chemical Compounds with Corresponding Key Targets

Compound	Key Target[a]	PDB ID[b]	Binding Energy/ (kcal/mol)
Quercetin	VEGFA	1BJ1	−4.22
	IL1B	2nvh	−6.13
	TNF	4twt	−4.88
	IL6	4ni7	−5.15
	CASP3	1rhj	−4.66
	AKT1	3o96	−6.48
	TP53	1gzh	−5.76
Kaempferol	TNF	4twt	−6.18
	CASP3	1rhj	−4.68
	AKT1	3o96	−6.85
β-sitosterol	CASP3	1rhj	−7.1

Abbreviation: [a]VEGFA, Vascular endothelial growth factor A; IL1B, Interleukin-1 beta; TNF, Tumor Necrosis Factor; IL6, Interleukin-6; CASP3, Caspase-3; AKT1, RAC-alpha serine/threonine-protein kinase; TP53, Cellular tumor antigen p53; [b]PDB ID, Identifiers in PDB Database.

Effect of PDB on Drosophila Development, Viability, and Fertility

Drosophila melanogaster was selected to determine whether PDB affects the normal growth, development, and reproductive capacity of living organisms. The results suggested that the white pupal curve and mean pupation time of larvae were not affected by supplementation with PDB extract in comparison with the control (Figures 5a and b), and no notable changes were observed in the viability or fertility of Drosophila adults treated with PDB (Figures 5c and d). These results indicate that PDB does not affect the development, viability, or fertility of *Drosophila*.

Effect of PDB on Glycolipid Metabolism Disorder in Diabetic Flies

An established diabetes *Drosophila* model (*Cg*>InR^{K1409A}) was employed, using the GAL4/UAS expression technique to selectively disrupt insulin receptor function in the adipose tissue of flies. This was achieved by genetically introducing the dominant-negative (DN) variant of InR (*UAS*-InR^{K1409A}), which in turn caused IR in *Drosophila*.[23] Consistent with previous findings, a considerable increase was observed in the circulating glucose and trehalose levels in the

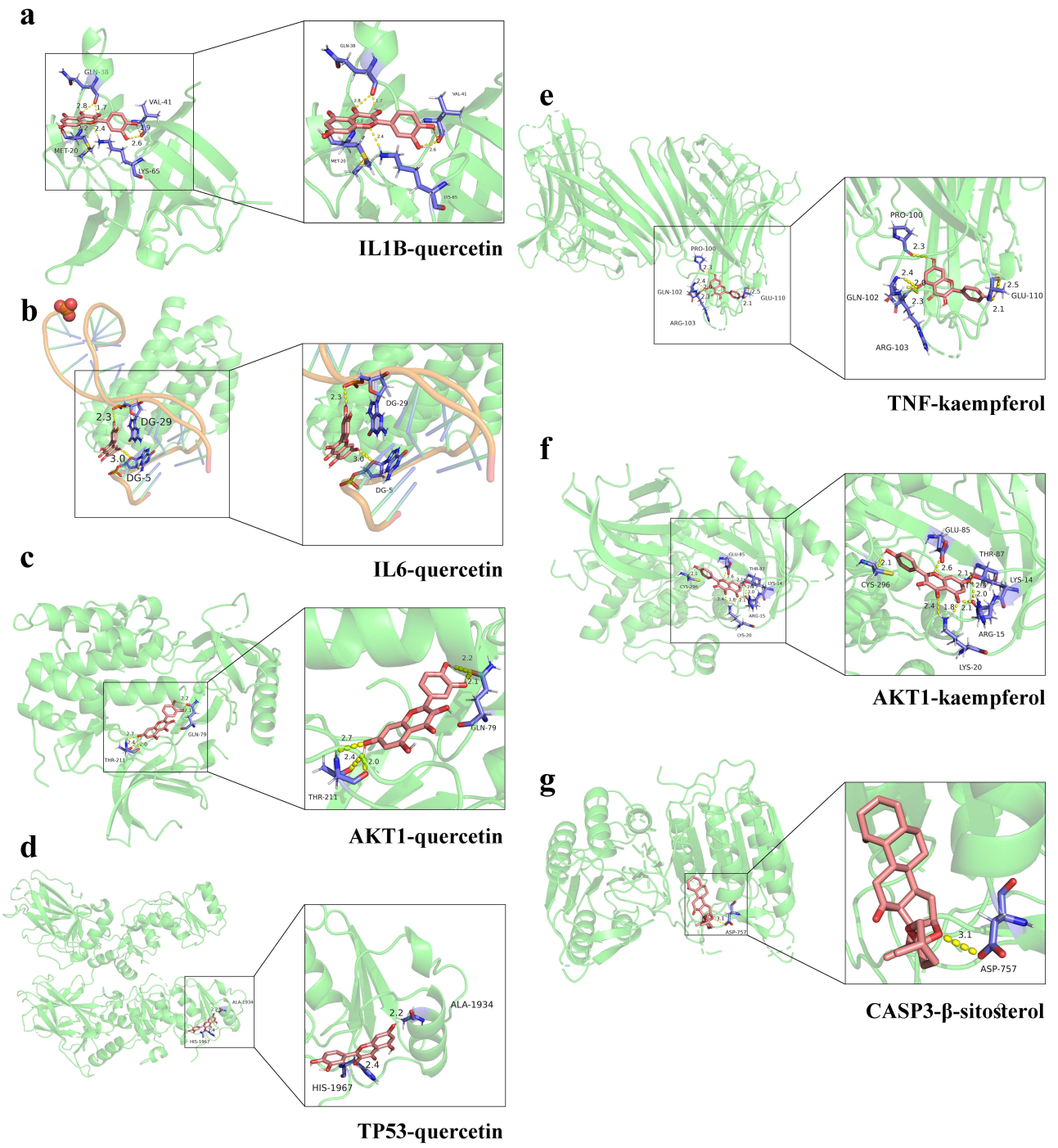

Figure 3 Docking conformation of active components and core target binding sites. Molecular docking of IL1B-quercetin (**a**), IL6-quercetin (**b**), AKT1-quercetin (**c**), TP53-quercetin (**d**), TNF-kaempferol (**e**), AKT1-kaempferol (**f**), and CASP3-β-sitosterol (**g**). Pink structures indicate chemical compounds; yellow dotted lines indicate hydrogen bonds, numbers indicate bond length, and blue structures indicate binding residues.

Cg>InR^{K1409A} diabetic fly model (Figure 6a and b). To further investigate the anti-diabetic effect of PDB, an extract was prepared and added to the medium fed to diabetic flies from egg to the third-instar larval stage. As expected, the increased hemolymph glucose and trehalose levels were largely inhibited by both PDB extract (Figure 6a and b) and Met (10 mM). The inhibitory effect was most notable in the 4.0 mg/mL PDB extract group.

Moreover, the larval protein content, body weight, and body size were decreased in the *Cg*>InR^{K1409A}-induced diabetes fly model (Figure 6c, e and g, Supplementary Figure 3), with substantial amelioration of body weight and size associated

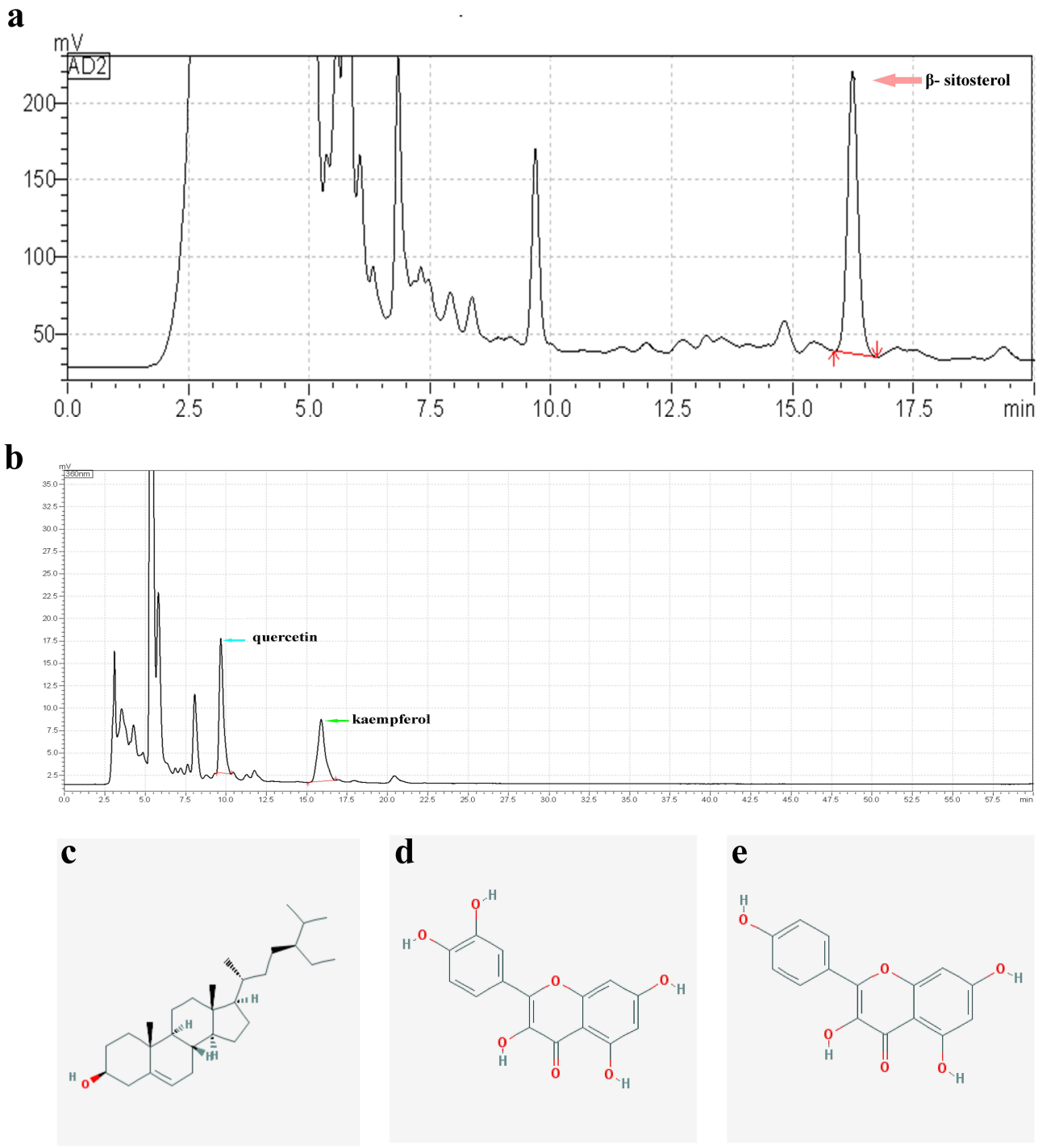

Figure 4 HPLC chromatogram of PDB. HPLC analysis of three chemical constituents, β-sitosterol (210 nm, **a**), quercetin (360 nm, **b**), and kaempferol (360 nm, **b**) in a sample of PDB. Obtained peaks are indicated by pink, blue, and green arrows. Molecular chemical formula of β-sitosterol (**c**), quercetin (**d**), and kaempferol (**e**).

with Met or 2.0, 4.0, 8.0, 16.0, and 32.0 mg/mL PDB (Figure 6e and g, Supplementary Figure 3). The protein content was unaffected. The reduced TAG contents of *Cg*>InR^{K1409A} were distinctly increased by Met, as well as 4.0 and 32.0 mg/mL PDB extracts, whereas treatment with 2.0, 8.0, and 16.0 mg/mL PDB had no effect (Figure 6d). The feed intake assay indicated no significant change in the ingestion rate among all groups (Figure 6f), excluding the possibility that different metabolic phenotypes are caused by changes in the feeding rate. Collectively, these results indicated that PDB could

Table 4 PDB Components and Relevant Characteristics[a]

Sample Name	Retention Time (min)	Area	Height	Concentration	Concentration Units	Proportion (%)
β-sitosterol	16.244	2,810,781	183,376	0.149	mg/mL	0.076
Quercetin	9.684	273,356	14,989	6.028	μg/mL	0.030
Kaempferol	5.055	905,660	59,919	5.047	μg/mL	0.025

Abbreviation: [a]PDB ID, *Potentilla discolor* Bunge.

ameliorate the *Cg*>InR^{K1409A}-triggered glycolipid metabolism disorder, including the increased circulating sugar level and the decreased body weight, body size, and lipid (TAG) content of *Drosophila*. A PDB extract of 4.0 mg/mL was therefore selected for further experimentation.

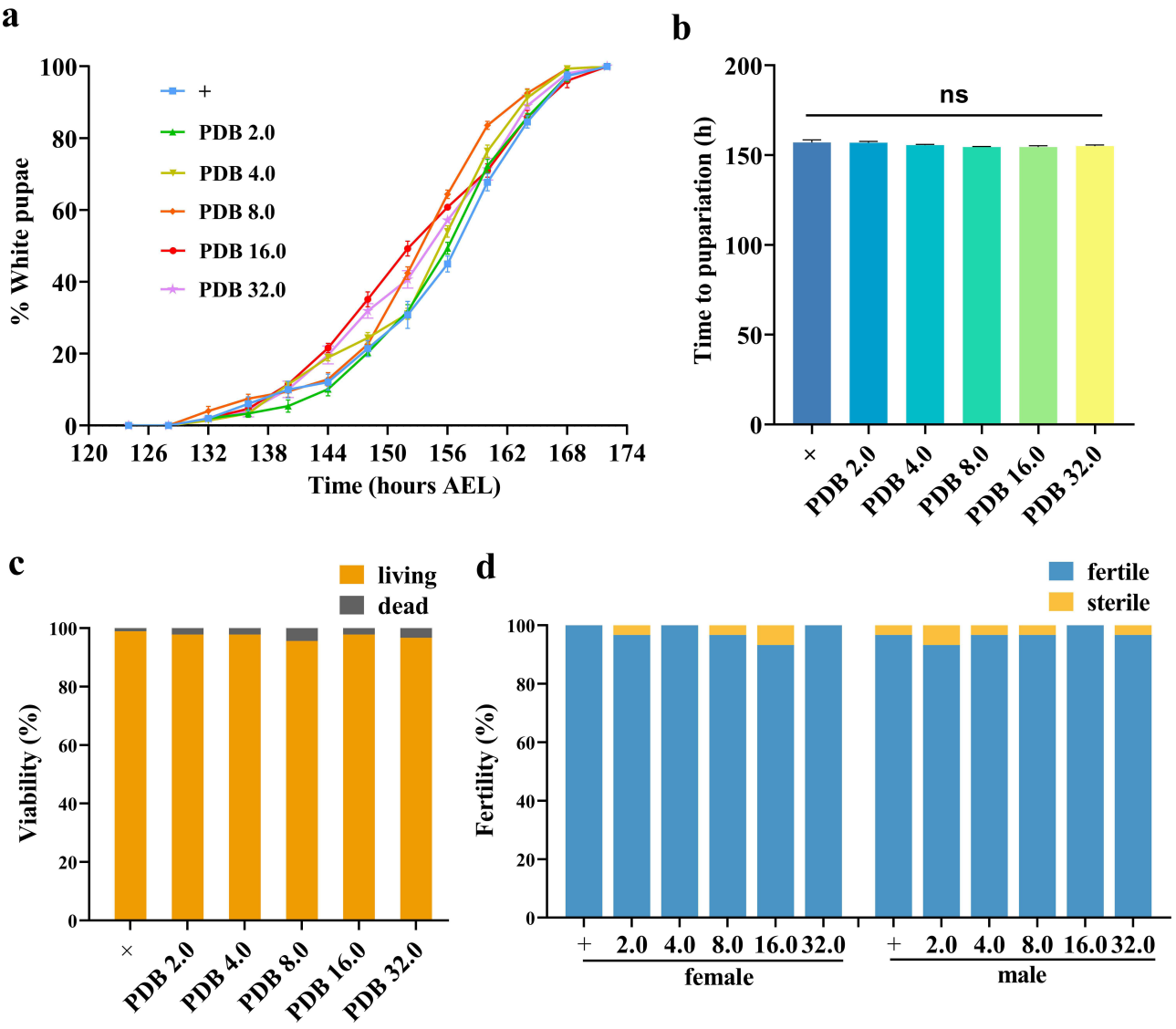

Figure 5 Effect of PDB on the development, viability, and fertility of *Drosophila*. Statistical analysis of the white pupae rate (**a**, n = 5) and time to pupariation (**b**, n = 5) of w^{1118} larvae fed normal food or PDB-treated food. For time to pupariation statistics, a one-way ANOVA with Bonferroni's multiple comparison tests was applied; ns indicates no significant difference. For the histogram of viability (**c**, n = 90) and fertility (**d**, n = 30) in w^{1118} adults, the chi-squared test was applied.

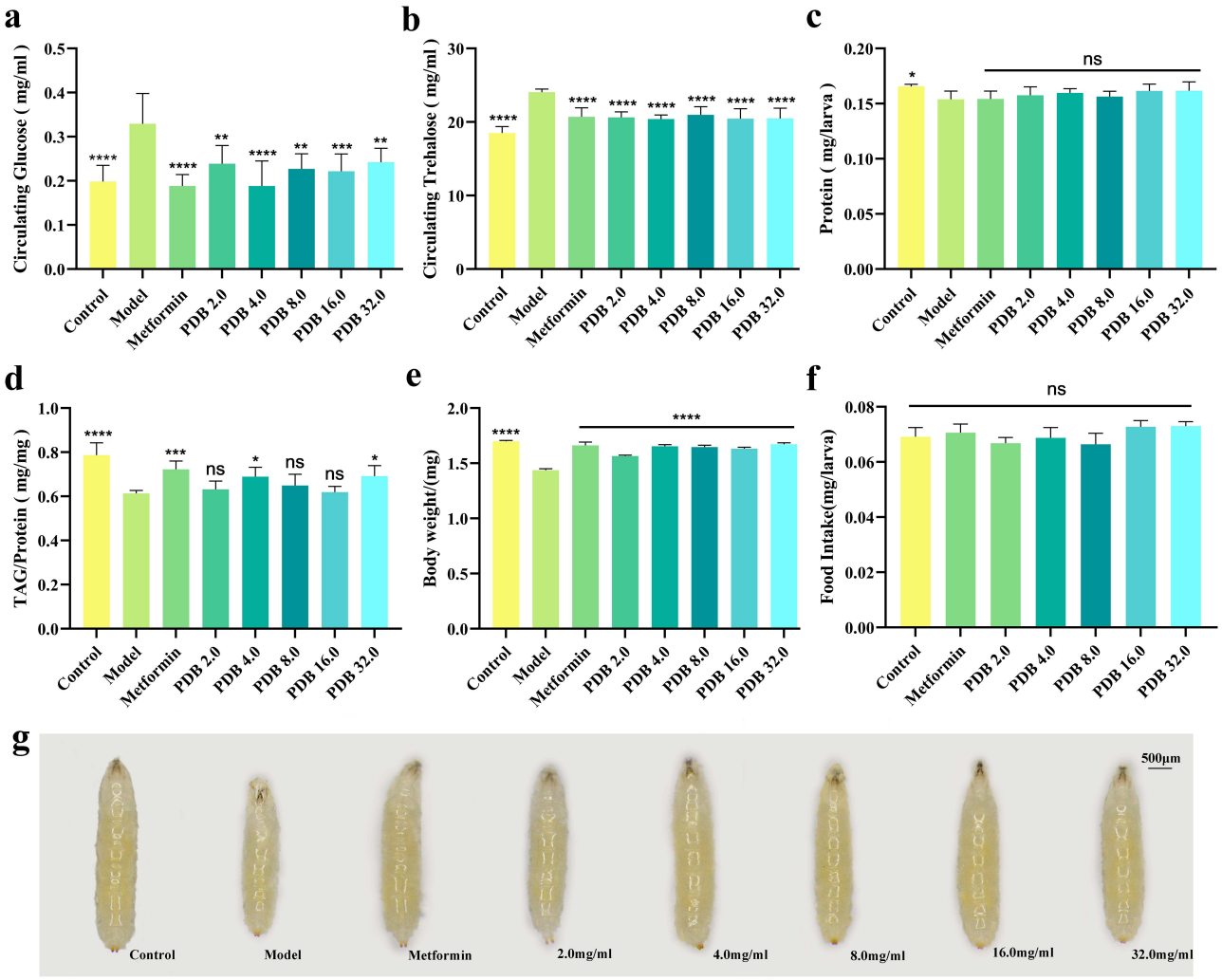

Figure 6 PDB ameliorates glycolipid metabolism disorder in diabetic flies. Assays for circulating metabolites were performed on third instar larvae: hemolymph glucose (**a**, 10–12 larvae per pool, n = 6), and hemolymph trehalose (**b**, 6–8 larvae per pool, n = 6). (**c**) Determination of protein content. The amount of protein indicates the soluble fraction in 0.05% PBST after heat inactivation (3 larvae per pool, n = 6). (**d**) Stored triglycerides (TAG) contents at larval stage relative to the protein contents of the sample to normalize the weight difference between control and other indicated groups (3 larvae per pool, n = 6). Column statistical charts of 3rd instar larvae body weight (**e**, n = 5) and food intake (**f**, 6–8 larvae per pool, n = 5). (**g**) Photographs showing larval body size. Scale bar, 500 μm. Error bars indicate standard deviation (SD). Statistical difference was calculated using one-way ANOVA and Bonferroni's multiple comparison test: ****P < 0.0001, ***P < 0.001, **P < 0.01, and *P < 0.05; ns: no significant difference.

Regulation of Akt Phosphorylation and CASP3 Expression in PDB Treatment

To further elucidate the action mechanism of PDB in the treatment of T2DM and IR based on the molecular docking results (Figure 3), two key targets, Akt and Caspase 3, were selected for validation. Firstly, Akt activity was monitored by checking its phosphorylation level via in vivo immunostaining and in vitro WB. As predicted, *Cg*>InR^{K1409A} promoted reduced Akt phosphorylation (p-Akt) levels at Ser505 (same as Ser473 in human Akt1) in the adipose tissue of flies with T2DM at the larval stage (Figure 7a, b, e, f, i, j, m, n and q–s), while total Akt levels were unchanged (Figure 7 and Supplementary Figure 4). The decrease in the p-Akt of *Cg*>InR^{K1409A} was moderately enhanced by Met or 4.0 mg/mL PDB (Figure 7c, d, g, h, k, l, o–s). However, the total Akt protein expression was unaffected by Met and PDB (Supplementary Figure 4). These results suggest that PDB improves Akt phosphorylation.

Next, we examined the CASP3 expression level in larval adipose tissue cells, as it is a key protease/effector caspase cascade initiator that induces extrinsic apoptosis. Compared with the control (Figure 8a, e, i and m), immunofluorescence staining results showed an increased CASP3 expression in the diabetes model (Figure 8b, f, j and n), significant

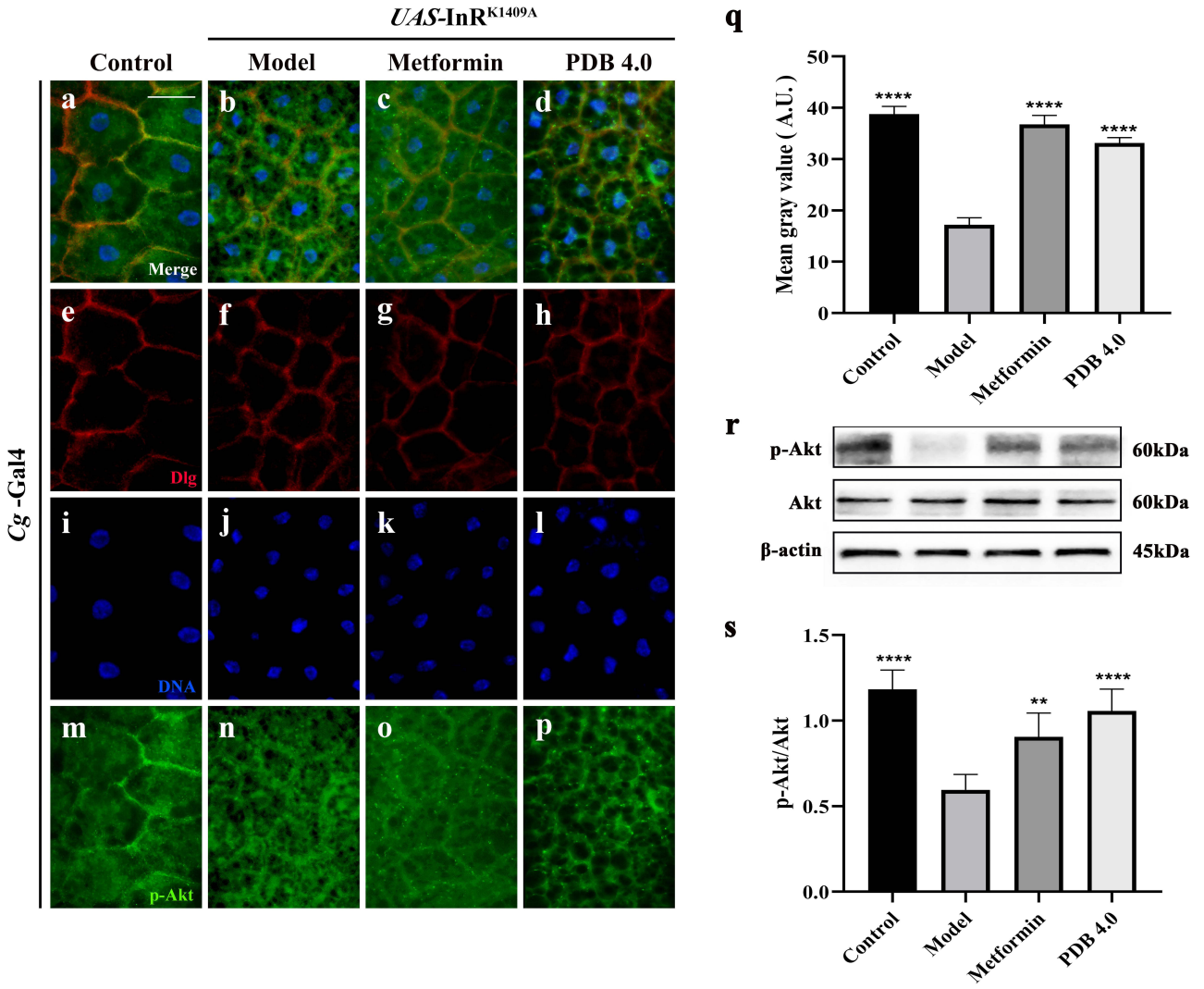

Figure 7 PDB increases Akt phosphorylation level. (**a–d**) Representative merged fluorescence micrographs showing *Drosophila* third-instar larval fat (body. Individual channels detecting only Dlg [red, (**e–h**)], only DAPI [blue, (**i–l**)], and only p-Akt [green, (**m–p**), fluorescent dots]. (**q**) Statistical analysis of the p-Akt fluorescence intensity in the indicated groups (n = 10). (**r**) Western blot analysis of whole-body extracts from third-instar larvae for phosphorylated Akt, total Akt, and β-actin (9 larvae per time); β-actin was used as a loading control. Groups (from left to right): Control (*Cg*-Gal4/+), Model (*Cg*-Gal4/+; *UAS*-InR^{K1409A}/+), Metformin (*Cg*-Gal4/+; *UAS*-InR^{K1409A}/+ files treated with 10 mM metformin), PDB (*Cg*-Gal4/+; *UAS*-InR^{K1409A}/+ files treated with 4 mg/mL PDB). **(s)** Statistical analysis of the p-Akt/Akt relative level (n = 5). The error bars indicate the SD. One-way ANOVA with Bonferroni's multiple comparison test was used to compute *P* values: ****$P < 0.0001$, and **$P < 0.01$. Scale bar, 20 μm.

suppression by PDB, and slight suppression by Met (Figure 8c, d, g, h, k, l, o, p and q). This indicates that PDB extract may suppress CASP3 activity to improve insulin resistance in *Drosophila* with T2DM.

Discussion

In recent decades, the number of people with diabetes has increased globally, with T2DM accounting for more than 90% of these cases.[29] T2DM is a chronic metabolic disorder with a high incidence rate, which is mainly characterised by IR caused by hyperglycaemia and insufficient insulin secretion.[30] It can lead to an increased risk of serious complications, especially the most prevalent microvascular and macrovascular complications including kidney disease, blindness, amputation, heart disease, and stroke.[31] Hence, there is an urgent need for the research and development of antidiabetic drugs with low toxicity and minimal side effects.

As a traditional herb, PDB has a long history of medicinal use with satisfactory drug efficacy in ameliorating diabetes and its complications.[10] In particular, in some provinces in southern China, people make tea directly from PDB for the treatment of T2DM.[32] Research has demonstrated that PDB has antibacterial, anti-inflammatory, antioxidant, and other

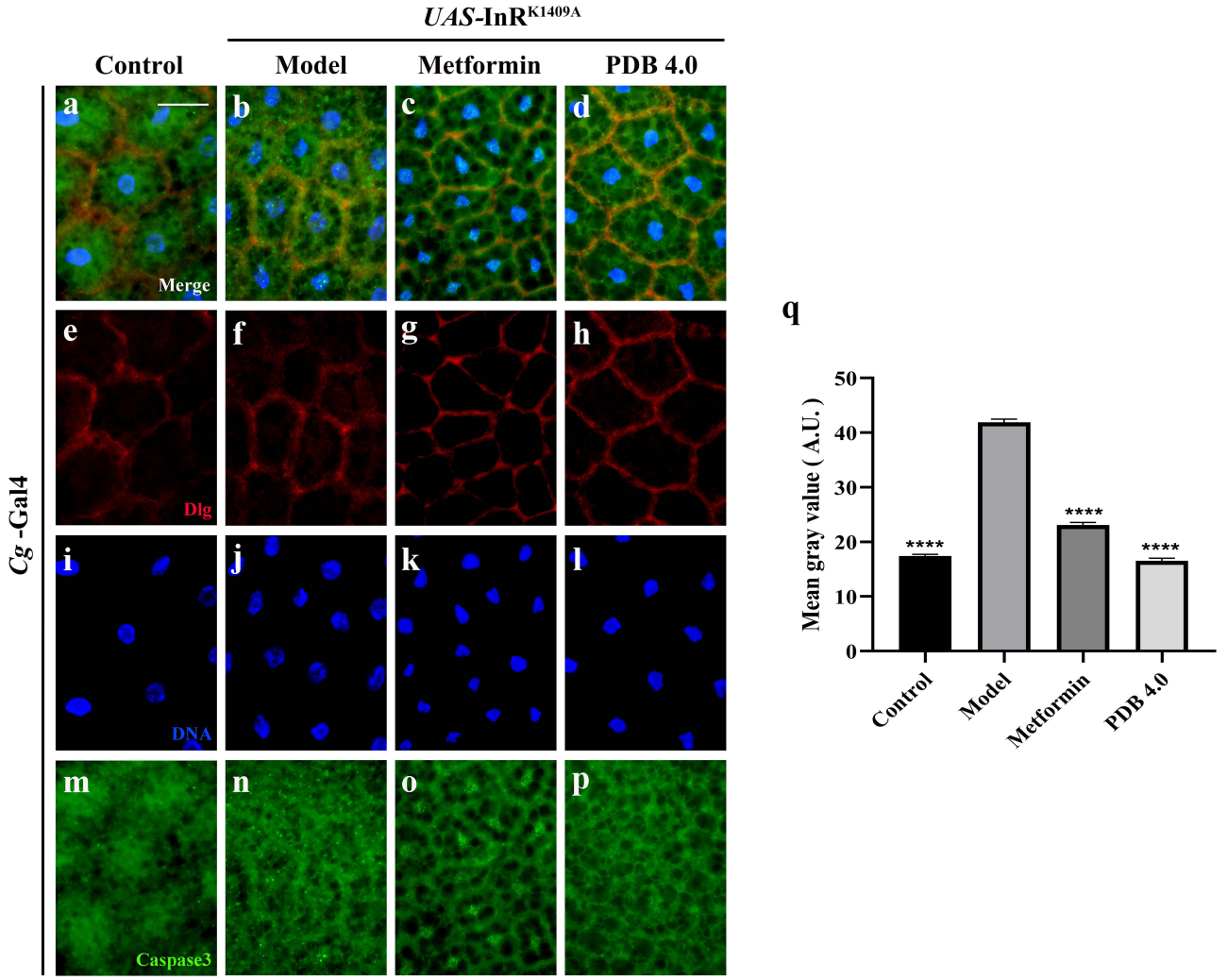

Figure 8 PDB reduces CASP3 expression. (**a–d**) Merged fluorescence micrographs of *Drosophila* third-instar larval fat body. Individual channels detecting only Dlg [red, (**e–h**)], only DAPI [blue, (**i–l**)], and only CASP3 [green, (**m–p**), fluorescent dots]. Groups (from left to right): Control (*Cg*-Gal4/+), Model (*Cg*-Gal4/+; *UAS*-InR^{K1409A}/+), Metformin (*Cg*-Gal4/+; *UAS*-InR^{K1409A}/+ files treated with 10 mM metformin), PDB (*Cg*-Gal4/+; *UAS*-InR^{K1409A}/+ files treated with 4 mg/mL PDB). (**q**) Statistical analysis of the CASP3 fluorescence intensity in indicated groups (n =10). Error bars indicate the SD. One-way ANOVA with Bonferroni's multiple comparison test was used to compute *P* values: ****$P < 0.0001$. Scale bar, 20 μm.

pharmacological effects.[33,34] Recently, Wang et al confirmed the therapeutic effect of the water extract of *Potentilla discolor* Bunge (PDW) in *Drosophila* on diabetes via JAK/STAT signalling.[35] Consistently, our research demonstrated the anti-diabetic effect of PDB in *Drosophila* with T2DM. However, the two studies differ as follows: 1) compared to the high-sugar diet (HSD)-induced T2DM fly model (dietary change), our work involved using the *Cg*>InR^{K1409A} diabetes *Drosophila* model (only modification of the genotype), thus in turn causing IR and establishing a diabetic model. Given the complexity of IR during T2DM occurrence and development, applying the *Cg*>InR^{K1409A} model could better elucidate the roles of IR in diabetes and screen potential drugs or ingredients; 2) in addition to animal experiments, our work involved network pharmacology and molecular docking analysis, which provides valuable insights into exploring the molecular mechanism of PDB in treating diabetes; 3) during drug extract preparation, Wang et al used distilled water as the carrier, whereas we first ground and soaked the PDB whole plant in 70% ethanol, then combined deionized water with the extract; 4) with regards to drug dosages, Wang et al used 0.02, 0.05, 0.1, and 0.2 g/mL PDW reserve solution to the HSD fly model, while our work utilised PDB dosages of 2.0, 4.0, 8.0, 16.0, and 32.0 mg/mL; and 5) regarding the molecular mechanism, our work uncovered that PDB may improve Akt phosphorylation and

suppress CASP3 activity to ameliorate insulin resistance in *Drosophila* with diabetes. Thus, our work on PDB provides a new experimental basis and mechanism for treating diabetes.

Herein, molecular docking analysis elucidated the three effective constituents (quercetin, kaempferol, and β-sitosterol) of PDB, possessing high binding activities with the core targets. Structurally, quercetin has two hydroxyl groups on the benzene ring, while kaempferol has only one; therefore, quercetin is slightly less hydrophobic than kaempferol. The hydrophobicity of β-sitosterol is much higher than that of quercetin and kaempferol. As shown in Table 3, the affinity of quercetin to CASP3 is slightly lower than that of kaempferol and much lower than that of β-sitosterol, which is consistent with the trend of hydrophobicity. The affinity of quercetin to the TNF/AKT1 protein is also slightly lower than that of kaempferol. Based on this, we speculate that the hydrophobicity of the drug may affect its binding activity with CASP3, which can provide valuable information for the structural modification and optimization of drug molecules in the future.

Among the active components of PDB, quercetin has been reported to have various pharmacological properties and a component of several plants. In addition, it is considered as one of the most widely used flavonoids to treat metabolic and inflammatory disorders,[36] with its anti-hyperglycemic effects enhancing insulin sensitivity, promoting glycogen synthesis, inhibiting α-glucosidase activity, and improving IR. Moreover, quercetin enhances glucose uptake in skeletal muscle by affecting glucose transport and insulin receptor signaling, thus improving glucose utilization.[37] Additionally, it can prevent diabetes by reducing oxidative stress, decreasing insulin-producing cell dysfunction, and enhancing insulin secretion from β-cells.[38] Kaempferol is a flavanol compound in diets and medicinal plants with antioxidant, anti-inflammatory, anti-tumor, anti-diabetic, and cardioprotective effects.[39] It protects against the chronic complications of T2DM by lowering blood glucose levels, improving the insulin sensitivity index, and maintaining normal blood lipid levels.[40] Previous studies demonstrate that the antidiabetic effects of kaempferol are mainly a consequence of three mechanisms: 1) improving insulin signaling and restoring the balance between glucose utilization and production, thereby improving glucose toxicity;[41,42] 2) regulating lipid metabolism and improving IR to reduce lipotoxicity;[43–45] and 3) restoring the autophagy–apoptosis imbalance to protect β cells. β-sitosterol, a sterol compound and a naturally effective antioxidant, has various functions, such as the regulation of cholesterol, and anti-inflammatory, analgesic, anti-tumor, anti-oxidative stress, and anti-diabetic effects.[46–48] Several studies suggest that β-sitosterol possesses antioxidant activity, thus functioning as a modest radical scavenger and physically as a membrane stabilizer.[49,50] As a scavenger of reactive oxygen species, β-sitosterol reduces oxygen free radicals and hydrogen peroxide levels and stimulates the enzymatic antioxidant which dependant on the activation of the oestrogen receptor/PI3K pathway.[51] Further, β-sitosterol has been proven to inhibit the intestinal absorption of cholesterol and elevate antioxidants, both enzymatic and non-enzymatic, making it an effective antidiabetic, hypolipidemic, neuroprotective, and chemopreventive agent. In this study, quercetin, kaempferol, and β-sitosterol were all present in the PDB extract, indicating that the anti-diabetic effect of PDB might be due to their synergistic effects, which needs further study.

Of the seven core PDB targets proteins identified for T2DM treatment, five were obtained via molecular docking analysis, namely IL1B, IL6, TP53, AKT1, and CASP3, of which IL1B is heavily involved in the pro-inflammatory process and highly associated with T2DM development.[52] TNF-α, an inflammatory factor, is associated with metabolic disorders and can alter insulin sensitivity, weaken insulin receptor signaling, reduce glucose transporter 4 in adipocytes, and inhibit adiponectin.[53] Further, IL6 is a pro-inflammatory cytokine that regulates cell differentiation, migration, proliferation, and apoptosis. Studies have shown that IL6 can induce the expression of SOCS-3 (insulin signaling inhibitor), which impairs insulin receptors and insulin receptor substrate-1 phosphorylation, leading to IR.[54] TP53 is known to respond to metabolic changes, affect metabolic pathways, and can be used as a novel therapeutic target to block cardiovascular and metabolic abnormalities associated with obesity.[55] The AKT protein is a core downstream factor of insulin/PI3K/AKT signalling,[56,57] is widely expressed in insulin-sensitive tissues, and can regulate glucose metabolism by inducing downstream molecules such as Glut to enhance glucose uptake.[58,59] Cell apoptosis is also an important factor in the development of diabetes, and CASP3, currently the most important executioner protein of the caspase cascade signal pathway, is widely used as a biomarker for apoptosis.[60,61]

Drosophila melanogaster is an invaluable model organism, offering insights into glucose and lipid metabolism disorders stemming from IR and T2DM.[23,62] Due to the superiority of the highly conserved circulatory system for maintaining the systemic sugar balance in flies and humans, we employed a well-established *Cg*>InR^{K1409A} diabetic *Drosophila* model to explore the therapeutic effect of PDB in T2DM. Based on quantification of *Drosophila* daily food

intake and the drug dose conversion between *Drosophila* and humans,[63–65] PDB extract was administered into the animal medium at concentrations of 2.0, 4.0, 8.0, 16.0, or 32.0 mg/mL, which were comparable to human treatment dosages of 4.17, 8.33, 16.67, 33.33, or 66.67 g/day, respectively. In our fly assay, the circulating glucose, trehalose, and triglyceride levels during the larval stage were evaluated. Remarkably, PDB displayed optimal inhibitory effects at 4 mg/mL, mirroring the therapeutic dose of 8.33 g/day in human patients, largely aligning with the recommended dosage range for humans in the Chinese Pharmacopoeia (9–15 g/day). These findings provide valuable insights into the clinical application of PDB in treating T2DM.

Conclusion

Building upon prior research, we integrated network pharmacology, molecular docking, and in vivo animal experiments to elucidate the active constituents, targets, and mechanisms underlying the efficacy of PDB in T2DM treatment. The results demonstrate that PDB ameliorates diabetes metabolism disorders by improving Akt activity and decreasing CASP3 expression at a concentration of 4 mg/mL in *Drosophila* (equal to 8.33 g/day for human patients). These findings provide information on key drug targets and crucial strategies for the clinical treatment of T2DM and related metabolic diseases.

Abbreviations

T2DM: type 2 diabetes mellitus; PDB: *Potentilla discolor* Bunge; IL1B: Interleukin-1 beta; IL6: Interleukin-6; AKT1: RAC-alpha serine/threonine-protein kinase; TP53: Cellular tumor antigen p53; TNF: Tumor necrosis factor; CASP3: Caspase-3; DM: diabetes mellitus; IR: insulin resistance; TCM: traditional Chinese medicine; InR: insulin receptor; OB: oral bioavailability; DL: drug-likeness; PPI: protein-protein interaction; GO: gene ontology; KEGG: Kyoto encyclopedia of genes and genomes; HPLC: high-performance liquid chromatography; PBS: phosphate-buffered saline; TAG: triglycerides; Blue-9: blue FCF; CST: Cell signaling technology; WB: Western blotting; VEGFA: Vascular endothelial growth factor A; PDW: water extract of *Potentilla discolor* Bunge; HSD: high-sugar diet.

Ethical Statement

Network pharmacology analysis utilized publicly available data and was approved by the Ethics Committee of North China University of Science and Technology. The use of *Drosophila melanogaster*, which are invertebrates, is not considered of ethical concern. The animal study was audited by the Laboratory Animal Welfare Ethics Committee of North China University of Science and Technology in accordance with the local legislation and institutional requirements.

Acknowledgments

We would like to thank the Bloomington *Drosophila* Stock Center for providing stock of *Drosophila melanogaster*, members of the Wu lab and Li lab, Dr. Zhen Chen (Oriental Herbs KFT of Hungary) for discussion and critical comments, and Editage (www.editage.cn) for English language editing. This work was supported by the Hebei Natural Science Foundation (H2022209027), Tangshan Science and Technology Project (21130230C) and Tangshan Talent Funding Project (A202203021) to Chenxi Wu, the Science and Technology Partnership Program, Ministry of Science and Technology of China (KY201904005) and Hebei Natural Science Foundation (H2023209038) to Ji-an Li, the Hebei Natural Science Foundation (H2022209031) to Hong Chang, and Graduate Student Innovation Fund of North China University of Science and Technology (2023S15) to Yinghong Li.

Author Contributions

All authors made a significant contribution to the work reported, whether that is in the conception, study design, execution, acquisition of data, analysis and interpretation, or in all these areas; took part in drafting, revising or critically reviewing the article; gave final approval of the version to be published; have agreed on the journal to which the article has been submitted; and agree to be accountable for all aspects of the work.

Disclosure

The authors report no conflicts of interest in this work.

References

1. Mizukami H, Kudoh K. Diversity of pathophysiology in type 2 diabetes shown by islet pathology. *J Diabetes Investig*. 2022;13:6–13. doi:10.1111/jdi.13679
2. Tinajero MG, Malik VS. An update on the epidemiology of type 2 diabetes: a global perspective. *Endocrinol Metab Clin North Am*. 2021;50:337–355. doi:10.1016/j.ecl.2021.05.013
3. Brown AE, Walker M. Genetics of insulin resistance and the metabolic syndrome. *Curr Cardiol Rep*. 2016;18:75. doi:10.1007/s11886-016-0755-4
4. National Pharmacopoeia Committee. *Chinese Pharmacopoeia*. Beijing: China Medical Science and Technology Press; 2020.
5. Mou JJ, Qiu S, Sun Y, et al. Study on chemical constituents from Potentilla discolor. *Chin Arch Trad Chin*. 2020;38:89–92.
6. Wang J, Jiao Q, Wang HB, et al. Research progress on chemical composition, quality evaluation and pharmacological activity of Potentilla discolor Bunge. *Chin Trad Pat Med*. 2016;38:1590–1593.
7. Xu X, Liu L, Huang JR. Recent advances study about chemical constituents, pharmacological effects and research prospects of potentilla discolor bunge. *Pharmacol Clin Chin Mater Med*. 2016;32:125–9+16.
8. Li T, Chang R, Zhang H, et al. Water extract of potentilla discolor bunge improves hepatic glucose homeostasis by regulating gluconeogenesis and glycogen synthesis in high-fat diet and streptozotocin-induced type 2 diabetic mice. *Front Nutr*. 2020;7:161. doi:10.3389/fnut.2020.00161
9. Li Y, Li JJ, Wen XD, et al. Metabonomic analysis of the therapeutic effect of Potentilla discolor in the treatment of type 2 diabetes mellitus. *Mol Biosyst*. 2014;10:2898–2906. doi:10.1039/C4MB00278D
10. Song C, Huang L, Rong L, et al. Anti-hyperglycemic effect of Potentilla discolor decoction on obese-diabetic (Ob-db) mice and its chemical composition. *Fitoterapia*. 2012;83(8):1474–1483. doi:10.1016/j.fitote.2012.08.013
11. Qin HW, Sun H, Wang HD, et al. Chemical constituents of Potentilla discolor. *J Chin Med Mater*. 2020;43:339–343.
12. Tan RR, Cong QY, Wang XM, et al. Effect of total flavonoids from Potentilla discolor on renovating islet β cell through adjusting GLP-1 mediated MAPK pathway. *Pharmacol Clin Chin Mater Med*. 2020;36:114–120.
13. Yamaguchi M, Yoshida H. Drosophila as a model organism. *Adv Exp Med Biol*. 2018;1076:1–10.
14. Rulifson EJ, Kim SK, Nusse R. Ablation of insulin-producing neurons in flies: growth and diabetic phenotypes. *Science*. 2002;296:1118–1120. doi:10.1126/science.1070058
15. Tennessen JM, Barry WE, Cox J, et al. Methods for studying metabolism in Drosophila. *Methods*. 2014;68:105–115. doi:10.1016/j.ymeth.2014.02.034
16. Pandey UB, Nichols CD. Human disease models in *Drosophila melanogaster* and the role of the fly in therapeutic drug discovery. *Pharmacol Rev*. 2011;63:411–436. doi:10.1124/pr.110.003293
17. He X, Gao X, Hong Y, et al. High fat diet and high sucrose intake divergently induce dysregulation of glucose homeostasis through distinct gut microbiota-derived bile acid metabolism in mice. *J Agric Food Chem*. 2024;72:230–244. doi:10.1021/acs.jafc.3c02909
18. Wang JB, Liu XR, Liu SQ, et al. Hypoglycemic effects of oat oligopeptides in high-calorie Diet/STZ-Induced diabetic rats. *Molecules*. 2019;24:558. doi:10.3390/molecules24030558
19. Nakitto AMS, Rudloff S, Borsch C, et al. *Solanum anguivi* Lam. fruit preparations counteract the negative effects of a high-sugar diet on the glucose metabolism in *Drosophila melanogaster*. *Food Funct*. 2021;12:9238–9247. doi:10.1039/D1FO01363G
20. Zhang R, Zhu X, Bai H, et al. Network pharmacology databases for traditional Chinese medicine: review and assessment. *Front Pharmacol*. 2019;10:123. doi:10.3389/fphar.2019.00123
21. Lin H, Wang X, Liu M, et al. Exploring the treatment of COVID-19 with Yinqiao powder based on network pharmacology. *Phytother Res*. 2021;35:2651–2664. doi:10.1002/ptr.7012
22. Consortium U. UniProt: the universal protein knowledgebase in 2021. *Nucleic Acids Res*. 2021;49(D1):1.
23. Cao X, La X, Zhang B, et al. Sanghuang tongxie formula ameliorates insulin resistance in drosophila through regulating PI3K/Akt Signaling. *Front Pharmacol*. 2022;13:874180. doi:10.3389/fphar.2022.874180
24. Wu Q, Du X, Feng X, et al. Chlordane exposure causes developmental delay and metabolic disorders in *Drosophila melanogaster*. *Ecotoxicol Environ Saf*. 2021;225:112739. doi:10.1016/j.ecoenv.2021.112739
25. Wang S, Wu C, Li Y, et al. Analysis of the anti-tumour effect of xuefu zhuyu decoction based on network pharmacology and experimental verification in drosophila. *Front Pharmacol*. 2022;13:922457. doi:10.3389/fphar.2022.922457
26. Li H, Tennessen JM. Methods for studying the metabolic basis of Drosophila development. *Wiley Interdiscip Rev Dev Biol*. 2017;6:10. doi:10.1002/wdev.280
27. Niu M, Zhang SQ, Zhang B, et al. Interpretation of the guidelines for network pharmacological evaluation methods. *Chin Trad Herb Drugs*. 2021;52:4119–4129.
28. Hans N, Gupta S, Patel AK, et al. Deciphering the role of fucoidan from brown macroalgae in inhibiting SARS-CoV-2 by targeting its main protease and receptor binding domain: in vitro and in silico approach. *Int J Biol Macromol*. 2023;248:125950. doi:10.1016/j.ijbiomac.2023.125950
29. Magliano DJ, Boyko EJ. IDF Diabetes Atlas. scientific committee. In: *IDF Diabetes Atlas*. Brussels: International Diabetes Federation; 2021.
30. Lee SH, Park SY, Choi CS. Insulin resistance: from mechanisms to therapeutic strategies. *Diabetes Metab J*. 2022;46:15–37. doi:10.4093/dmj.2021.0280
31. Forbes JM, Cooper ME. Mechanisms of diabetic complications. *Physiol Rev*. 2013;93:137–188. doi:10.1152/physrev.00045.2011
32. Zhang L, Yang J, Chen XQ, et al. Antidiabetic and antioxidant effects of extracts from potentilla discolor bunge on diabetic rats induced by high fat diet and streptozotocin. *J Ethnopharmacol*. 2010;132:518–524. doi:10.1016/j.jep.2010.08.053
33. Kong XN, Cui HY, Zhou HL. Hypoglycemic effect of total flavonoids from potentillae discoloris herba in type 2 diabetic db/db mice. *Chin J Exp Trad Med Formulae*. 2021;27:78–84.
34. Liu Y, Fu QH, Shi MN, et al. Mechanism of Potentilla discolor in treating UC by regulating mitochondrial autophagy. *China J Chin Mater Med*. 2021;46:3907–3914.

35. Li Y, Wang J, Xu Y, et al. The water extract of Potentilla discolor Bunge (PDW) ameliorates high-sugar diet-induced type II diabetes model in *Drosophila melanogaster* via JAK/STAT signaling. *J Ethnopharmacol*. 2023;316:116760. doi:10.1016/j.jep.2023.116760
36. Anand David AV, Arulmoli R, Parasuraman S. Overviews of biological importance of quercetin: a bioactive flavonoid. *Pharmacogn Rev*. 2016;10:84–89. doi:10.4103/0973-7847.194044
37. Hamilton KE, Rekman JF, Gunnink LK, et al. Quercetin inhibits glucose transport by binding to an exofacial site on GLUT1. *Biochimie*. 2018;151:107–114. doi:10.1016/j.biochi.2018.05.012
38. Shi GJ, Li Y, Cao QH, et al. In vitro and in vivo evidence that quercetin protects against diabetes and its complications: a systematic review of the literature. *Biomed Pharmacother*. 2019;109:1085–1099. doi:10.1016/j.biopha.2018.10.130
39. Egbuna C, Awuchi CG, Kushwaha G, et al. Bioactive compounds effective against type 2 diabetes mellitus: a systematic review. *Curr Top Med Chem*. 2021;21:1067–1095. doi:10.2174/1568026621666210509161059
40. Kitakaze T, Jiang H, Nomura T, et al. Kaempferol promotes glucose uptake in myotubes through a JAK2-dependent pathway. *J Agric Food Chem*. 2020;68:13720–13729. doi:10.1021/acs.jafc.0c05236
41. Li H, Ji HS, Kang JH, et al. Soy Leaf extract containing kaempferol glycosides and pheophorbides improves glucose homeostasis by enhancing pancreatic β-cell function and suppressing hepatic lipid accumulation in db/db mice. *J Agric Food Chem*. 2015;63:7198–7210. doi:10.1021/acs.jafc.5b01639
42. Tang H, Zeng Q, Tang T, et al. Kaempferide improves glycolipid metabolism disorder by activating PPARγ in high-fat-diet-fed mice. *Life Sci*. 2021;270:119133. doi:10.1016/j.lfs.2021.119133
43. Torres-Villarreal D, Camacho A, Castro H, et al. Anti-obesity effects of kaempferol by inhibiting adipogenesis and increasing lipolysis in 3T3-L1 cells. *J Physiol Biochem*. 2019;75:83–88. doi:10.1007/s13105-018-0659-4
44. Ochiai A, Othman MB, Sakamoto K. Kaempferol ameliorates symptoms of metabolic syndrome by improving blood lipid profile and glucose tolerance. *Biosci Biotechnol Biochem*. 2021;85:2169–2176. doi:10.1093/bbb/zbab132
45. Tie F, Ding J, Hu N, et al. Kaempferol and kaempferide attenuate oleic acid-induced lipid accumulation and oxidative stress in HepG2 cells. *Int J Mol Sci*. 2021;22:8847. doi:10.3390/ijms22168847
46. Babu S, Jayaraman S. An update on β-sitosterol: a potential herbal nutraceutical for diabetic management. *Biomed Pharmacother*. 2020;131:110702. doi:10.1016/j.biopha.2020.110702
47. Gumede NM, Lembede BW, Brooksbank RL, et al. β-sitosterol shows potential to protect against the development of high-fructose diet-induced metabolic dysfunction in female rats. *J Med Food*. 2020;23:367–374. doi:10.1089/jmf.2019.0120
48. Babu S, Krishnan M, Rajagopal P, et al. Beta-sitosterol attenuates insulin resistance in adipose tissue via IRS-1/Akt mediated insulin signaling in high fat diet and sucrose induced type-2 diabetic rats. *Eur J Pharmacol*. 2020;873:173004. doi:10.1016/j.ejphar.2020.173004
49. Yoshida Y, Niki E. Antioxidant effects of phytosterol and its components. *J Nutr Sci Vitaminol*. 2003;49:277–280. doi:10.3177/jnsv.49.277
50. Gupta R, Sharma AK, Dobhal MP, et al. Antidiabetic and antioxidant potential of β-sitosterol in streptozotocin-induced experimental hyperglycemia. *J Diabetes*. 2011;3:29–37. doi:10.1111/j.1753-0407.2010.00107.x
51. Vivancos M, Moreno JJ. beta-Sitosterol modulates antioxidant enzyme response in RAW 264.7 macrophages. *Free Radic Biol Med*. 2005;39:91–97. doi:10.1016/j.freeradbiomed.2005.02.025
52. Jiao J, Wang Z, Guo Y, et al. Association between IL-1B (−511)/IL-1RN (VNTR) polymorphisms and type 2 diabetes: a systematic review and meta-analysis. *PeerJ*. 2021;9:e12384. doi:10.7717/peerj.12384
53. Akash MSH, Rehman K, Liaqat A. Tumor necrosis factor-alpha: role in development of insulin resistance and pathogenesis of type 2 diabetes mellitus. *J Cell Biochem*. 2018;119:105–110. doi:10.1002/jcb.26174
54. Akbari M, Hassan-Zadeh V. IL-6 signalling pathways and the development of type 2 diabetes. *Inflammopharmacology*. 2018;26:685–698. doi:10.1007/s10787-018-0458-0
55. Sliwinska A, Kasznicki J, Kosmalski M, et al. Tumour protein 53 is linked with type 2 diabetes mellitus. *Indian J Med Res*. 2017;146:237–243. doi:10.4103/ijmr.IJMR_1401_15
56. Huang X, Liu G, Guo J, et al. The PI3K/AKT pathway in obesity and type 2 diabetes. *Int J Biol Sci*. 2018;14:1483–1496. doi:10.7150/ijbs.27173
57. Savova MS, Mihaylova LV, Tews D, et al. Targeting PI3K/AKT signaling pathway in obesity. *Biomed Pharmacother*. 2023;159:114244. doi:10.1016/j.biopha.2023.114244
58. Wang J, Chu H, Li H, et al. A network pharmacology approach to investigate the mechanism of erjing prescription in type 2 diabetes. *Evid Based Complement Alternat Med*. 2021;2021:9933236. doi:10.1155/2021/9933236
59. Yin B, Bi YM, Fan GJ, et al. Molecular mechanism of the effect of huanglian jiedu decoction on type 2 diabetes mellitus based on network pharmacology and molecular docking. *J Diabetes Res*. 2020;2020:5273914. doi:10.1155/2020/5273914
60. Luo XL, Luo WJ, Li M, et al. Cardioprotective effect of liraglutide combined with growth differentiation factor-11 recombinant protein on db/db diabetic mice and its effect on TGF-β1, PPARγ and Caspase-3. *Chin J Gerontol*. 2019;39:5085–5088.
61. Jiang M, Qi L, Li L, et al. The caspase-3/GSDME signal pathway as a switch between apoptosis and pyroptosis in cancer. *Cell Death Discov*. 2020;6:112. doi:10.1038/s41420-020-00349-0
62. Meng Q, Xu Y, Li Y, et al. Novel studies on *Drosophila melanogaster* model reveal the roles of JNK-Jak/STAT axis and intestinal microbiota in insulin resistance. *J Drug Target*. 2023;31:261–268. doi:10.1080/1061186X.2022.2144869
63. Deshpande SA, Carvalho GB, Amador A, et al. Quantifying Drosophila food intake: comparative analysis of current methodology. *Nat Methods*. 2014;11:535–540. doi:10.1038/nmeth.2899
64. Slack C, Alic N, Foley A, et al. The ras-Erk-ETS-signaling pathway is a drug target for longevity. *Cell*. 2015;162:72–83. doi:10.1016/j.cell.2015.06.023
65. Wang S, Wu F, Ye B, et al. Effects of xuefu zhuyu decoction on cell migration and ocular tumor invasion in drosophila: XFZYD affects cell migration and tumor invasion. *BioMed Res Int*. 2020;2020:1–13.